ELSEVIER

Evaluation of an Improved Version of SAIL Model for Simulating Bidirectional Reflectance of Sugar Beet Canopies

B. Andrieu, F. Baret,† S. Jacquemoud,§ T. Malthus,** and M. Steven‡*

The processing of remote-sensing data requires simple but accurate models of directional reflectance of the vegetation canopy. In this study, a reflectance model for a homogeneous canopy is evaluated over an extensive set of radiometric measurements performed on sugar beet canopies. The model corresponds to the Scattering by Arbitrary Inclined Leaves (SAIL) model (Verhoef, 1984) in which the term for first order scattering is corrected for hot-spot and leaf specular reflectance. Leaf optical properties are calculated using the PROSPECT model (Jacquemoud and Baret, 1990). Experimental data correspond to a two-year experiment and express a large variability of leaf area index, chlorophyll concentration and soil background optical properties. In the first data set, reflectance was measured about midday under vertical viewing in five optical Thematic Mapper bands. In the second data set, both vertical and oblique measurements (zenith angle 45°, four azimuth angles) were performed from sunrise to sunset in the three SPOT bands. Except for leaf cuticle reflectance, structure and optical variables were measured in the field or adjusted to field measurement, independently of reflectance calculations. Although the structure of sugar beet canopies departs strongly from a turbid medium, a good agreement with measurements was obtained in the case of vertical, north and south view directions. However, the model underestimated the measurements close to the hot-spot direction. In the near infrared, there was also some underestimation of canopy reflectance in the opposite direction to the hot-spot. Possible reasons for these differences are discussed. ©*Elsevier Science Inc., 1997*

* INRA Bioclimatologie, Thiverval-Grignon, France
† INRA Bioclimatologie, Montfavet, France
§ GPS, Université de Paris, Paris, France
** Department of Geography, University of Edinburgh, Edinburgh, Scotland
‡ Department of Geography, University of Nottingham, Nottingham, United Kingdom

Address correspondence to Dr. Bruno Andrieu, INRA Bioclimatologie, 78850 Thiverval-Grignon, France.
Received 20 July 1995; revised 22 June 1996

INTRODUCTION

In recent years, large efforts have been made to improve the ability of simple models to predict the directional reflectance of vegetation canopies with a minimum number of input parameters. The inclusion of leaf specular reflectance (Vanderbilt and Grant, 1985; Ross and Marshak, 1989) and of the effect of finite leaf dimension on bidirectional gap fraction (Kuusk, 1985, 1991; Marshak, 1989; Myneni and Kanemasu, 1988; Qin and Jupp, 1993; Qin and Xiang, 1994) represent probably the most significant progress in this area. The SAIL model (Verhoef 1984, 1985), has been shown to be a good level of compromise between simplicity and accuracy. Jacquemoud (1993) coupled it to the PROSPECT model for leaf optical properties (Jacquemoud and Baret, 1990) and Kuusk introduced his hot-spot correction (Kuusk, 1985). In an earlier paper (Jacquemoud et al., 1995), we evaluated inversion of this model from nadir measurements. Here specular reflectance also is included. The model will be denoted further as the SPK model; it is close to Kuusk's multispectral canopy reflectance model, (Kuusk, 1994), with some differences in the parameterizations used in the calculations, which will be detailed later.

Models have frequently been evaluated over crops with relatively small or narrow leaves, such as wheat or barley. On the other hand, few experiments have evaluated models over a very large range of canopy conditions, and particularly for crop structures very different from that of cereals. For these reasons, we performed an extensive two-year reflectance experiment on sugar beet

REMOTE SENS. ENVIRON. 60:247–257 (1997)

655 Avenue of the Americas, New York, NY 10010

0034-4257/97/$17.00
PII S0034-4257(96)00126-5

canopies, in which a large range of independent variations of soil and leaf optical properties, canopy structure, and sun-sensor geometry was obtained. Sugar beets are quite compact, low plants with broad leaves. Thus canopy structure departs strongly from a turbid medium. Furthermore, model validation sometimes uses fitting of the input variables or parameters that are difficult to measure directly. This process may lead to an optimistic evaluation of model accuracy and dissimulate model or measurement errors because the actual value of a variable can be different from the value corresponding to the best fit. An important effort was made here to measure or estimate canopy structure and optical properties independently from radiometric measurements.

MATERIAL AND METHOD

Calculation of Canopy Reflectance

The SAIL and PROSPECT models and the principle of hot-spot correction have been described in the literature cited in the Introduction: thus we give only the information required to present the modifications that we specifically introduced.

The SAIL model computes light transfer inside the canopy through three differential equations describing the relations between the incident solar flux that has not undergone any interaction (E_s), and the upward (E_+) and downward (E_-) diffuse fluxes, assumed to be hemispherical. For calculation of reflectance, a fourth differential equation describes the contribution of the leaves illuminated by the three preceding fluxes to the flux toward the observer and the attenuation of this flux along the path. This leads to a system of four differential equations:

$$\begin{aligned} dE_s/dz &= k_s E_s \\ dE_-/dz &= -sE_s + aE_- - \sigma E_- \\ dE_+/dz &= s' E_s + \sigma E_- - aE_+ \\ dE_o/dz &= \omega E_s + vE_- + \mu E_+ - k_o E_o \end{aligned} \quad (1)$$

The coefficients of these equations are calculated from leaf area density (μ_l), leaf normal orientation distribution (*lad*) and leaf reflectance and transmittance; see Verhoef (1985) for detailed calculations.

Hot-Spot

The model includes the hot-spot correction of (Kuusk, 1985, 1991) for the contribution to reflectance of first-order scattering. The correction depends on the parameter s_l which represents the apparent size of leaves. Kuusk (1991) proposed the following approximation to take into account the effect of *lad* and view zenith angle on the apparent size of circular leaves

$$s_l[\Omega_o, g_l(\Omega_l)] = \frac{\pi d_l G(\Omega_o)}{4\mu_o} \Big/ \int_{2\pi} \frac{g_l(\Omega_l)}{2\pi} \frac{d\Omega_l}{\sqrt{1+\tan^2\theta_l \sin^2\varphi_l}} \quad (2)$$

Here $\Omega_o=(\theta_o,\varphi_o)$ is the direction toward the observer, $\Omega_l=(\theta_l,\varphi_l)$ is the leaf normal orientation, d_l is the ratio between leaf diameter and canopy height; $g_l(\Omega_l)$ is the leaf normal orientation distribution, $G(\Omega_o)$ is the mean projection of unit leaf area on the plane normal to Ω_o, and $\mu_o=\cos(\Omega_o)$.

In Eq. (2), the term $G(\Omega_o)/\mu_o$ represents the extinction coefficient for the view angle. Actually, the view direction Ω_o and the incident direction Ω_s play symmetrical roles in the angular autocorrelation of the leaf indicator function. Furthermore, for a canopy with broad leaves, the hot-spot effect is significant even for large differences between incident and viewing directions. Thus we used a symmetrized expression for s_l:

$$s_l[\Omega_o,\Omega_s,g_l(\Omega_l)] = \sqrt{s_l(\Omega_o,g_l(\Omega_l)]\cdot s_l[\Omega_s,g_l(\Omega_l)]} \quad (3)$$

Sugar beet leaves may be acceptably considered disc shaped, so we estimated d_l from the mean area of leaves. To make the computation faster, we derived an analytical approximation for the integral term of Eq. (2). This approximation holds for an ellipsoidal leaf normal orientation distribution (Campbell 1986), without significant error for mean leaf zenith angle between 0° and 85° ($r^2=0.9992$, $stde=0.025$). It reads:

$$\left(\int_{2\pi} \frac{g_l^{\text{elliptical}}(\Omega_l)}{2\pi} \frac{d\Omega_l}{\sqrt{1+\tan^2\theta_l \sin^2\varphi_l}}\right)^{-1} \approx 1+0.357\left(\frac{\langle\theta_l\rangle}{1.693-\langle\theta_l\rangle}\right)^{1.252}, \quad (4)$$

where $\langle\theta_l\rangle$ is the mean zenith angle of the leaf normal orientation distribution.

Leaf Specular Reflectance

In the SPK model, the leaf area density is assumed to be independent of z, and the contribution of first-order scattering from foliage elements to canopy Bidirectional Reflectance Distribution Function (BRDF) is calculated as:

$$R^1 = \omega \cdot \int_0^H p(z,\Omega_s,\Omega_o)dz, \quad (5)$$

where $p(z,\Omega_s,\Omega_o)$ is the bidirectional gap fraction at level z and the coefficient ω is related to Ross's area scattering phase function Γ (Ross, 1981): $\omega=\Gamma\, u_l(\mu_s\mu_o)^{-1}$. Thus, including the specular contribution requires ω to be calculated as $\omega=\omega_d+\omega_s$, where 1) ω_d is calculated from the bilambertian component of leaf reflectance ρ_d and from leaf transmittance and 2) ω_s is the contribution due to the specular component of leaf reflectance: $\omega=\Gamma_{spec}\, u_l(\mu_s\mu_o)^{-1}$. The area scattering phase function for specular reflectance Γ_{spec} is calculated according to Vanderbilt and Grant (1985) and Nilson (1991) :

$$\Gamma_{spec} = 0.125 \cdot g_l(\Omega_l^*) \cdot K \cdot F(a,n), \quad (6)$$

where Ω_l^* is the direction of leaf normal giving specular reflectance (i.e. the bisector of the angle between Ω_s and

Table 1. Spectral Bands of the Radiometers

Channel	*xs1*	*xs2*	*xs3*	*TM4*	*TM5*
wavelength (nm)	500–590	620–680	790–890	1550–1750	2080–2350

Ω_0); $F(\alpha,n)$ is the Fresnel factor for a material of refractive index n and a ray of incidence α relative to the leaf normal; K is an empirical parameter, which is required because the actual specular reflectance of a leaf is generally found to be less than that calculated from Fresnel equations.

In the PROSPECT model, leaf cuticle reflectance is assumed to be lambertian: it is calculated from Fresnel equations for incoming light isotropic within a cone of direction of aperture α_0 and independent of leaf orientation. Jacquemoud and Baret (1990) found that the value $\alpha_0=59°$ was a compromise enabling the model to predict at best the normal-hemispherical reflectance as measured by spectrophotometry. The fraction of rays refracted by the cuticle causes volume reflectance and transmittance. Here we estimated ρ_d as the leaf volume reflectance calculated by PROSPECT from the light refracted through the cuticle for incident directions within a cone of aperture 59°. For calculating the other coefficients of Eq. (1), we used the standard calculation of leaf optical properties by PROSPECT.

Treatment of Diffuse Sky Radiance

The hot-spot correction and the leaf specular reflectance are considered only for the contribution of first-order scattering to canopy BRDF; they are not included in diffuse flux calculations. In particular, they are not taken into account in the calculation of the reflectance of diffuse incoming radiation. However, for canopies with large leaves, the hot-spot effect may increase canopy BRDF from 20% to 40% for a large range of directions. On the other hand, cuticle reflectance may represent 20% to 50% of total leaf reflectance for visible light. Thus we computed the reflectance of sky radiance by numerical integration of bidirectional reflectance and compared it with the estimate by the two-stream approximation.

Experiment

Design of the Experiment

A two-year experiment was performed in Broom's Barn (England) in July 1989 and in Grignon (France) in July 1990. Both experiments were performed with sugar beet crops and aimed to provide a large range of states of canopy and background reflectance.

In the Broom's Barn experiment, different canopy structures (three sowing dates, two measurement dates, three sowing densities, four levels of thinning) were combined with contrasted background reflectances (natural soil, peat, sand, white and black paper). We attempted to create variations in leaf chlorophyll content by artificial infection of some plots with Yellow Beet Virus. However, chlorosis remained moderate at the time of the reflectance experiments, and only differences in canopy structure and background reflectance were significant. Altogether the data set represents 120 combinations of canopy and background conditions. Leaf area index ranged from 0.2 to 5.5, and intermediate values were obtained from varied growth stages and population densities. Thinning enabled the modulation of row structure effects: thinning every second plant within the rows made the row structure nearly vanish, whereas thinning every second row reinforced the row structure. The different backgrounds enabled us to obtain a large range of background reflectances in each spectral band (see Table 2).

Canopy BRDF was measured for vertical viewing in the three bands of SPOT, using a Cimel radiometer with a circular ifov of 12°, and in the two middle infrared Thematic Mapper (TM) bands, using a Barringer Hand Held Ratioing Radiometer (HHRR) with a rectangular ifov of 12° by 24°. Corresponding wave bands are given in Table 1. Radiance data were averaged over a 2 m transect representing about 1 m^2. Cimel data were cali-

Table 2. Background Reflectances Measured for Vertical Direction and a Solar Zenith Angle of 30°

Location	*Background*	*xs1*	*xs2*	*xs3*	*TM4*	*TM5*
Broom's Barn	Natural soil	0.14	0.20	0.27	0.40	0.39
	Peat (dry)	0.03	0.04	0.11	0.30	0.21
	Peat (wet)	0.02	0.02	0.06	0.13	0.07
	Sand	0.28	0.36	0.47	0.62	0.59
	Black paper	0.06	0.08	0.70	0.76	0.54
	White paper	0.95	0.94	0.92	0.78	0.40
Grignon	Natural soil	0.13	0.19	0.25	0.35	
	Black cloth	0.02	0.02	0.03	0.07	
	White cloth	0.81	0.80	0.81	0.77	

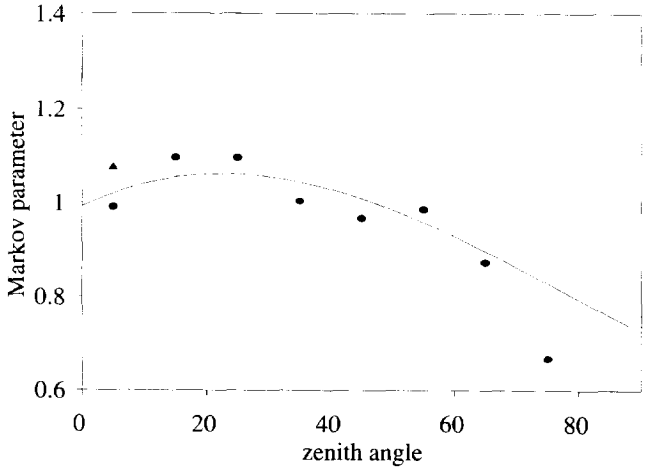

Figure 1. Angular course of the Markov parameter: circle, Broom's Barn, 1989; triangle, Grignon, 1990.

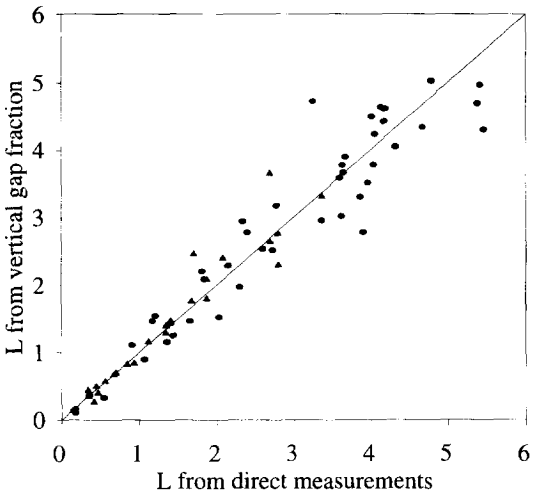

Figure 2. Leaf area index estimated from direct measurement and from vertical gap fraction: circle, Broom's Barn, 1989; triangle, Grignon, 1990.

brated to reflectance by continuously monitoring a reference panel of known BRDF with a second radiometer. For calibration of the HHRR data, an integrating sphere was used to measure the incoming radiance immediately before and after each target measurements. The cosine response of the integrating sphere was calibrated against the reference panel. Measurements were performed between 9h30 and 15h (solar time), corresponding to a range in solar zenith angles between 29° and 45°.

In Grignon, canopy structure variations (two sowing densities, four levels of thinning) were combined with contrasted background reflectance (natural soil, black and white cloths), and variations of leaf optical properties induced by small doses of metsulfuron herbicide spray (one control treatment and two levels of herbicide treatment). Leaf area indices ranged from 0.3 to 3.3 and artificial backgrounds provided a wide range of background reflectances in all wave bands (Table 2). Herbicide treatment resulted not only in strong chlorosis, but also in modifications of leaf orientation and in a more diffuse aspect of the leaves.

A first set of reflectance measurements was made under vertical viewing in the three SPOT bands and in TM4. Measurements were performed between 9h to 15h (solar time) corresponding to solar zenith angle variation between 23° and 47°. A second set of measurements consisted in monitoring the BRDF of all plots every half hour throughout a day, from sunrise to sunset, under vertical viewing and under oblique viewing (θ_0=45°) for four azimuth directions (north, east, south and west). This second set of measurements will be denoted further as the "Spider" experiment. It was performed over the natural soil background only, using 5 Cimel radiometers, each instrument sampling between 1 m^2 and 2 m^2 of the target surfaces. The Grignon data and the Broom's Barn data were calibrated in similar fashion.

Solar position was computed from classical relations, using time and the geographic position of the measurements. The ratio E_d/E_t between diffuse and total irradiance was continuously monitored in the three Cimel bands, using a radiometer to measure total radiation and a second radiometer with an equatorial ring to measure diffuse radiation. Nearly all measurements were performed under a totally clear sky, so the diffuse fraction came only from sky scattering. The diffuse fraction was

Table 3. Mean Leaf Zenith Angle Estimated from Field Measurements

	Sowing Dates 1 and 2	*Sowing Date 3*
Broom's Barn		
Low sowing density	46°	40°
Normal and high sowing density	57°	40°
	Reference Treatment	*Herbicide Treatments*
Grignon		
Normal sowing density	52°	36°
High sowing density	52°	33°

typically in the range of 0.18 for xs1 and 0.07 for xs3. However it was significantly higher at low solar elevations, with maximum values in the range of 0.30 for xs1 and 0.18 for xs3, for measurements close to sunrise and sunset. To estimate E_d/E_t in the middle-infrared bands, we used the measurements in the three Cimel bands to adjust two parameters a and x of the relation $E_d/E_t=a\lambda^x$. The diffuse component so obtained for the middle-infrared bands was always very low (less than 0.03), and thus an accurate estimate was unnecessary.

Simulation of the Bands of the Radiometer

The reflectance for the bands of the radiometer were calculated as a weighted average of reflectances simulated for 15 to 20 wavelengths for SPOT bands and 40 wavelengths for TM bands. The weights fit the spectral sensitivity of the radiometer.

Measurement of Canopy Structure

Leaf Normal Orientation Distribution

Leaf zenith angle was measured as a function of leaf rank for individual beets, using a hand-held clinometer. Independently, leaf area was measured as a function of leaf rank for five beets of each plot. The mean leaf zenith angle was calculated from these two functions and was used to approximate the *lad* by an elliptical distribution (Campbell, 1986). Accuracy of these estimates is limited by the accuracy of individual leaf orientation measurements and by the small sample on which these measurements were performed, owing to the difficulty of the method (six beets in Broom's Barn, eight beets in Grignon). Consequently, we did not try to estimate the *lad* of each individual plot, rather we tried to describe the main trends. Results are presented in Table 3. Data measured on normal density plots are consistent with those given by Hodanova (1972) for a similar stage of beet development. Interplot variations are consistent with the visual aspect of the plots. In particular, the herbicide treatment in Grignon resulted in strong wilting of the leaves.

Directional Gap Fraction

The directional gap fraction, $Po(\theta)$, was measured in Broom's Barn by digital analysis of downward-looking hemispherical photographs. Together with *lad* and leaf area index (*lai*) measurements, directional gap fraction was used to estimate a Markov parameter $\lambda(\theta)=\log[Po(\theta)]/\log[Po^*(\theta)]$ Nilson, 1971); here $Po(\theta)$ is the measured gap fraction and $Po^*(\theta)$ is the gap fraction calculated for a random turbid medium of the same *lai* and *lad*. These data are presented in Baret et al. (1993). However, in that paper, *lai* was estimated from laminae area only. Here we also took into account the area of petioles. A unique function, $\lambda(\theta)$, was found to be satisfactory, independent of population and stage of development. As shown by Figure 1, we found some angular variations of the Markov parameter. However, for zenith angles between 0° and 45°, the gap fraction calculated for a random turbid medium matches the measured gap fraction reasonably; for zenith angles larger than 50°, the gap fraction is probably underestimated. Considering the characteristic structure of sugar beet canopies, $Po(\theta)$ is not expected to be described exactly by the usual approximation of a turbid medium.

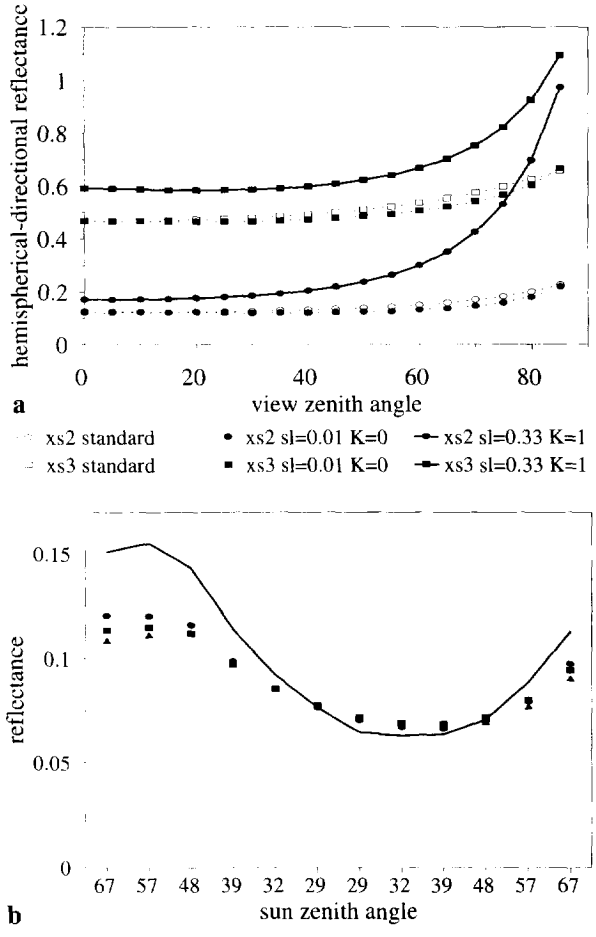

Figure 3. a) Reflectance of isotropic sky radiance: numerical integration against standard approximation. *lai*=10; s_1 and *K* given in the figure; other vegetation parameters correspond to the non-herbicide treatment. A scale factor of 4 is applied to xs2. b) Comparison of methods for taking into account sky radiance: diurnal evolution of reflectance in channel xs1 for east view direction. Solid line, measured; square, numerical integration; triangle, two-stream; circle, sun only.

Table 4. Mean Chlorophyll Concentration and Interplot Standard Deviation ($\mu g/cm^2$)

Broom's Barn		*Grignon*		
Reference	*Yellow Beet Virus*	*Reference*	*Herbicide 1*	*Herbicide 2*
35±2	31±2	34±2	23±1	15,5±1

Leaf Area Index

Direct measurements of laminae area were performed by removing the plants over an area of 1.5 m^2 on each plot. A subsample of five plants was used to estimate the leaf area per unit fresh weight of laminae. The total lamina area was then calculated from the fresh weight of all laminae in the 1.5-m^2 sample. The area of petioles was estimated from photographs of leaves. Petioles were considered cylindrical elements, and their efficient area was estimated as $\pi/2$ times their projected area (Lang, 1993). The efficient area of petioles represented about 18% of the area of laminae.

The direct measurements of laminae area could not be performed at the exact place where radiometric measurements were made. Consequently, in addition to hemispherical photographs, ordinary vertical photographs were taken to measure the gap fraction corresponding to the exact area where radiometric measurements were performed. Leaf area index was also estimated from the measured vertical gap fraction and the measured *lad*. Figure 2 shows that direct and indirect estimates of *lai* are in good agreement. We believe that, for *lai* less than 3, differences are mainly due to plot heterogeneity. For higher values of *lai*, the relative accuracy of gap fraction measurement decreases, which results in larger errors in the estimates of leaf area index. Finally, the relation between vertical gap fraction, *lai* and *lad* appears very stable and independent of population, stage of development, or herbicide treatment. In the Grignon experiment, plots showed some spatial heterogeneity, thus indirect estimates were thought to be more representative of the canopy over which the reflectance measurements were made and so were used for the simulations.

Leaf Size Parameter

Photographs of leaves were also used to estimate the parameter d_l from the Grignon experiment. The height of the canopy was measured with a meter rule. Finally, the value d_l=0.42 was taken for all plots. The parameter s_l was estimated from Eq. (2) to (4).

Soil and Leaf Optical Properties

Soil Reflectance

As with the SAIL model, our model requires three parameters for soil reflectance: The bidirectional soil reflectance $\rho_s(Q_s,\Omega_0)$ and the directional-diffuse soil reflectances $\rho_s(hem,\Omega_s)$ and $\rho_s(hem,\Omega_0)$. The bidirectional reflectances of bare soil and artificial backgrounds were measured for the same geometric conditions as those for the sugar beet plots. This was important mostly for the Spider experiment, where strong variations (typically, in a ratio 2.5:1) in bidirectional soil reflectance were observed in relation to sun-sensor geometry. However, the directional-diffuse reflectances were not measured but were approximated as the bidirectional reflectance measured for vertical viewing at a solar zenith angle of 30°.

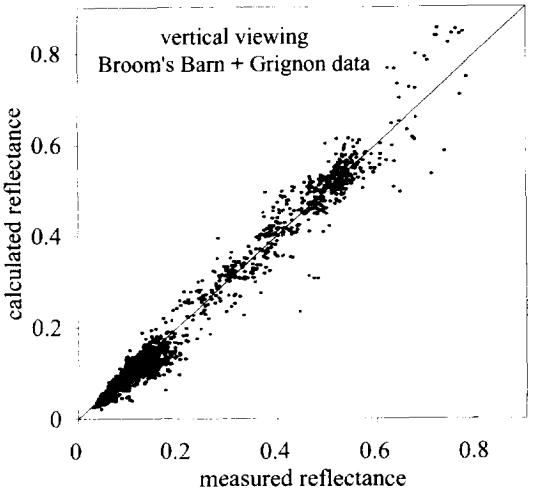

Figure 4. Plot of measured versus simulated reflectance for θ_0=0°, with all conditions of soil and vegetation taken together. Broom's Barn, 1989 (five spectral bands), and Grignon, 1990 (four spectral bands).

Table 2 shows the range of variations of background reflectance.

Leaf Optical Properties

Leaf optical properties were calculated with PROSPECT, using measured or estimated surface concentrations of chlorophyll (C_{ab}), carotenoids (C_{xc}), water (C_w), and the leaf structure parameter (N).

C_{ab} and C_{xc} were estimated from digital analysis of photographs of leaves made in the laboratory (Andrieu et al. 1992). A relation between C_{ab}, C_{xc}, and leaf optical properties was established from simulations with PROSPECT, parameters were adjusted on control samples, and then the relation was applied to a large area of leaves, using digitized photographs to estimate reflectance of large samples of leaves. This method was chosen because direct measurement of C_{ab} and C_{xc} are very time consuming and could not have been performed on samples large enough to be representative at the plot level. Consistent with visual observation, there was no noticeable effect of Yellow Beet Virus contamination in the Broom's Barn experiment, but herbicide treatments in Grignon resulted in marked chlorosis (Table 4).

Water concentration in leaf lamina, C_w was estimated for each plot by drying 50 leaf disks taken by using a cork borer. Values estimated at the plot level typically ranged between 30 and 45 mg/cm^2. The leaf structure parameter, N, was adjusted so that PROSPECT estimated at best the measured ratio between leaf reflectance and transmittance in the near infrared. A constant value N=1.5 was taken for both experiments. Finally, the parameter K, for specular reflectance, was the only parameter that was adjusted in relation to the measurement of reflectance of the plots. Consistent with the visual aspect of the leaves, only two different values of

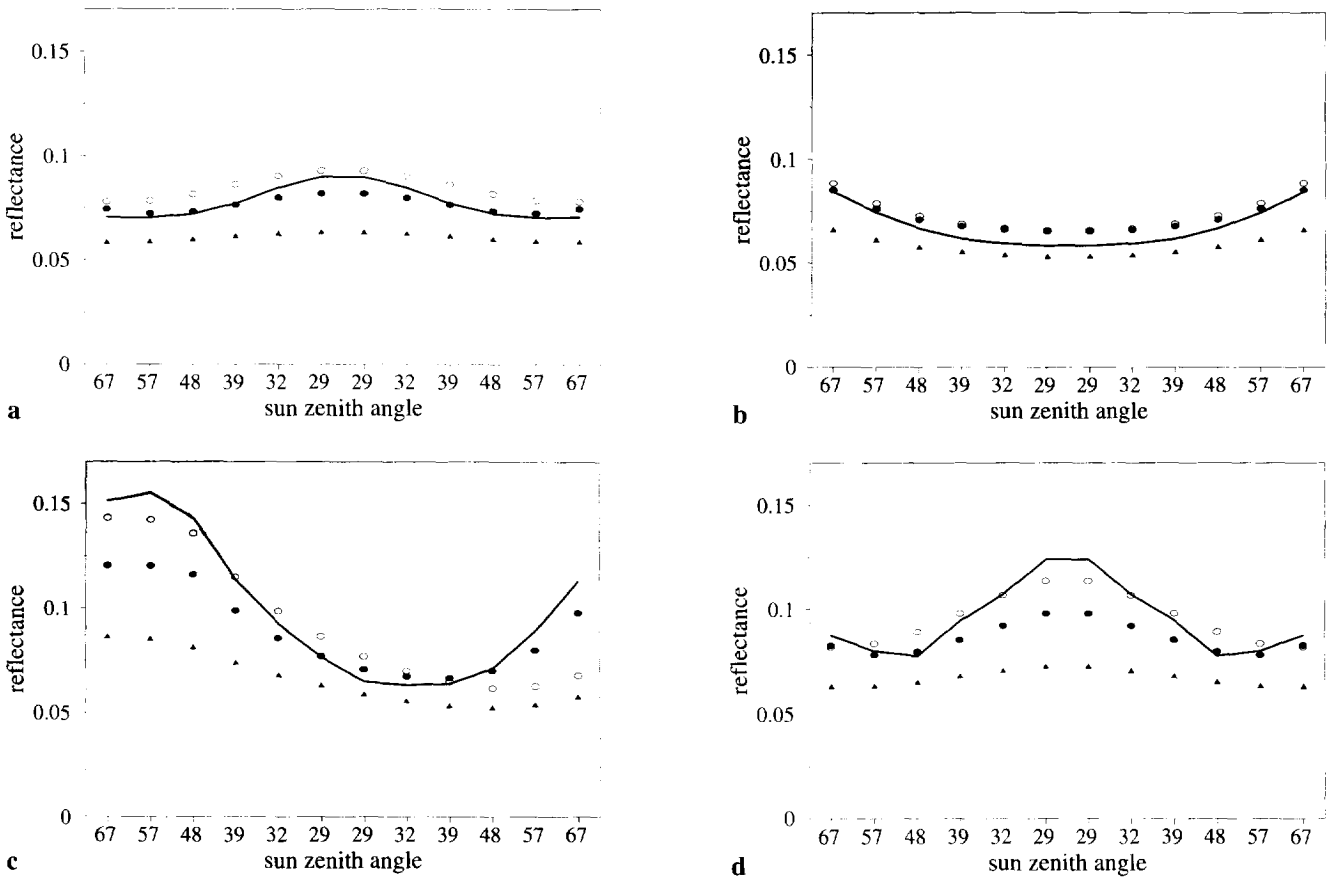

Figure 5. Diurnal evolution of reflectance for xs1: a) θ_0=0°; b) θ_0=45° north; c) θ_0=45° east-west; d) θ_0=45° south. North, south, and so forth, are directions from the target to the radiometer. Figure (c) corresponds to the east azimuth, with time increasing from left to right on the x axis, and to the west azimuth, with time increasing from right to left. Solid line, measured; triangle, SAIL; open circle, SPK (d_1=0.42, K=0); solid circle, SPK (d_1=0.42, K=1).

K were allowed: one for the plots in Broom's Barn and the nonherbicide treatment in Grignon: and the other for the herbicide treatments in Grignon, which resulted in visual alteration of leaf cuticle.

Optical properties of petioles were also estimated by using the PROSPECT model. In the visible, petiole reflectance was close to that of the laminae of herbicide treatment 2; thus C_{ab} was fixed to 15 μg/cm^2. C_w and N were estimated as 4.8 times their value for laminae; this corresponds to the ratio between surfacic fresh weight of petioles and laminae. Because their optical properties are quite different from those of leaves and they represent a noticeable efficient area, sugar beet petioles are a significant element and should be taken into account, as are the stems in cereal (see, e.g., Qin, 1993).

Finally, the optical properties required for the coefficient of Eq. (1) were calculated as an average of optical properties of laminae and petioles, weighted by their efficient area.

RESULTS AND DISCUSSION

To evaluate the usefulness of computing reflectance of sky radiance by numerical integration, we considered the case of an isotropic sky radiance (i.e., the hemispherical-directional reflectance factor). Integration was performed for different numbers of point sources, and results did not depend strongly on the number of point sources when it was more than 30. This is consistent with the smooth shape of the hotspot due to the large size of sugar beet leaves (see below). Figure 3a compares hemispherical-directional reflectance calculated from numerical integration with standard calculations using the two-stream approximation, for a thick canopy (lai=10). When hot-spot and leaf specular reflectance are negligible, the difference between standard calculations and numerical integration is low. In our conditions (s_1≈0.33, K=1), estimates from the two-stream approximation are about 20% (xs3) or 30% (xs2) lower than those using numerical integration for view directions close to vertical. However, this difference increases markedly for view zenith angles larger than 60°, especially in the xs2 channel.

Figure 3b shows a better agreement of our measurements with the use of the numerical integration than with using the two-stream approximation; however, the best agreement was obtained when the diffuse fraction was not taken into account. We believe that this is because a large part of the diffuse fraction of radiation

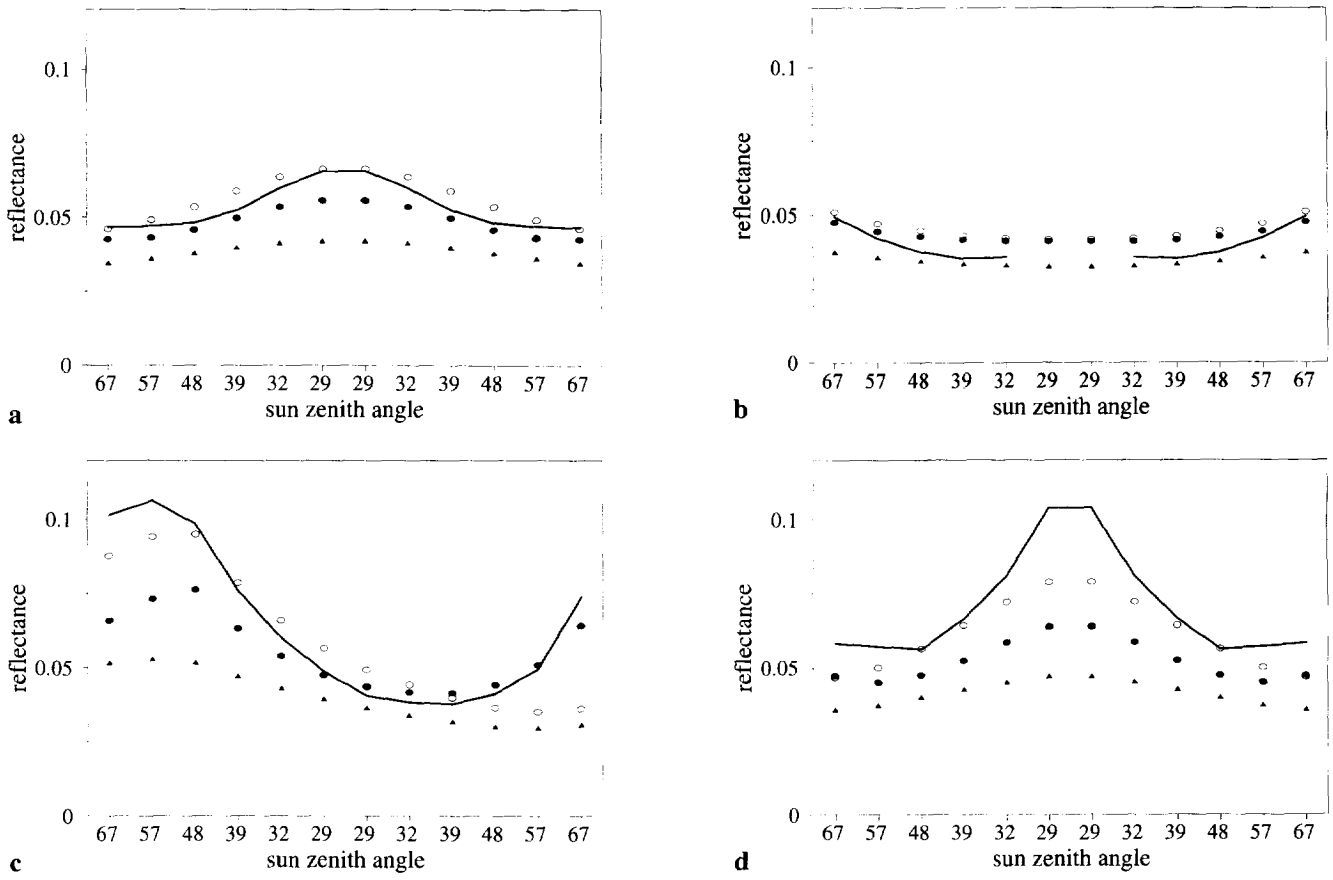

Figure 6. Diurnal evolution of reflectance for xs2 (notations as in Fig. 5).

came from a narrow cone around the sun and not from the whole hemisphere. The differences due to the different methods of calculating the skylight contribution were always low compared with the differences between simulated and measured reflectances. Thus, results will be presented without taking into account the diffuse fraction. Finally, numerical integration is probably a significant feature for short wavelengths and a very turbid atmosphere, but a realistic directional function of sky radiance is then required.

Figure 4 plots the simulated reflectance against the measured reflectance, for nadir viewing, considering all measurements together. For the treatment of the leaf specular component, a value of $K=1$ is taken here for green plots and $K=0.3$ for the herbicide treatment. This difference is in accordance with the visual aspects of the leaves, which presented a glossy appearance in the green treatments. The standard deviation between estimated and measured reflectance is 0.03, which is apparently within the expected range, given the accuracy associated with the biophysical and radiometric measurements. We checked that each wavelength was simulated with approximately the same relative accuracy.

The diurnal variation in reflectance over natural soil from the Spider experiment is presented in Figures 5a–5d (xs1), Figures 6a–6d (xs2), and Figures 7a–7d (xs3). To show the main features of diurnal variations, the data were averaged in two ways :

1. Reflectance measurements were averaged for six nonherbicide-treated plots with a mean leaf area index of 2.6.
2. Given the north-south orientation of rows, measurements for similar view-sensor geometry obtained in the morning and in the evening also were averaged.

Simulations are shown for both the SAIL and SPK models, with or without taking into account the specular component. Table 5 gives sun zenith and azimuth as a function of solar time. The large value of the d_1 parameter ($d_1=0.42$) estimated for sugar beet canopies leads to a broad angular range for the hot-spot effect. Thus, the SPK model gave, in all wave bands, reflectance estimates higher than those of the SAIL model, even for sun directions very different from the view direction.

The SPK model matched the diurnal variations of reflectance in the visible region for most sun-sensor geometries, except those close to the hot spot. A specular component of leaf reflectance was required to obtain good agreement in the direction opposite to the hot spot,

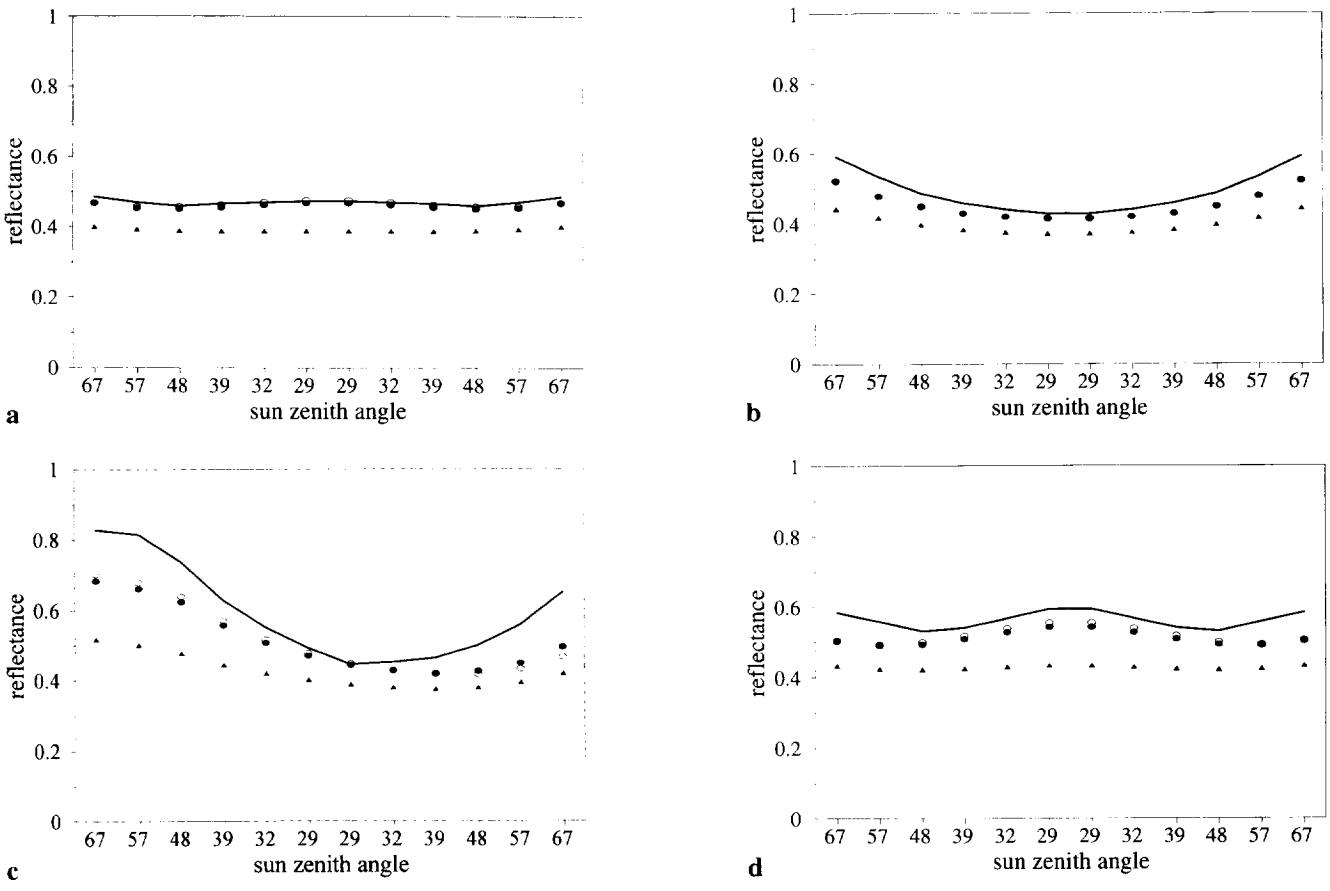

Figure 7. Diurnal evolution of reflectance for xs3 (notations as in Fig. 5).

but it resulted in an underestimate in the hot-spot direction. This can be seen for east-, west-, and south-view azimuths and, to a lesser extent for nadir viewing about noon. It is in relation with our procedure for estimating the diffuse component of leaf reflectance, which imposes the leaf hemispherical reflectance to be that predicted by PROSPECT. Usually, the correction for the specular component is computed only as an additive term to leaf hemispherical reflectance, which is not correct. Adopting this approach would have produced better agreement in the hot-spot direction but an overestimate of canopy reflectance for other sun-sensor geometries.

In the near infrared, the relative difference between measured and calculated reflectances is lower than in the visible. Differences are important mostly for east- or west-view directions and low solar elevations. However, Figures 5, 6, and 7 show that the model tends to underestimate reflectance for sun-sensor geometries close to the hot spot and for geometries where the specular component is important in the visible. Computation of multiple scattering by the two-stream approach is known to be a rough approximation. Moreover, the sugar beet canopy, made of quite compact plants with broad leaves, quite obviously violates the assumption of a turbid medium. However, the similarity between the underestimates for the near infrared and those for visible wavelengths suggests that the multiple scattering approximation may not be the main cause of the underestimations observed in the near infrared. Several other sources may have contributed:

1. Errors in biophysical and radiometric measurements have greater consequences at low solar elevations and for sun-sensor geometries corresponding to the antihot-spot direction. In these conditions, canopy reflectance is very sensitive to

Table 5. Sun Position and Solar Time (Sun Azimuth Is Relative to South)

Solar time	*06:54*	*07:44*	*08:39*	*09:38*	*10:32*	*11:25*	*12:19*	*13:16*	*14:10*	*15:19*	*16:15*	*17:16*
Sun azimuth	−96	−87	−76	−61	−44	−23	+5	+31	+52	+71	+83	+95
Sun zenith	67	59	50	41	34	29	28	31	37	47	56	66

lad, which was not measured with high accuracy. Furthermore, calibration of radiometric data is less accurate at low solar elevations.

2. The hypothesis of an isotropic leaf volume reflectance is a crude approximation of the actual bidirectional reflectance pattern of leaves. Data produced by Ross (1981), Breece and Holmes (1971), Walter, Shea et al. (1989), and Sanz (1994) show that leaf reflectance has a strong directional diffuse component, even in the near infrared. This may explain part of the difference observed in the direction opposite to the hot spot, similar to what is observed in the visible when the leaf specular component is not taken into account. Furthermore, ray-tracing simulations (Govaerts et al., 1996) show that a hot-spot feature may occur at the leaf level; thus the area scattering phase function for the hot-spot direction may be underestimated when using the approximation of a lambertian+specular leaf reflectance.
3. Direct measurements have shown that the actual directional gap fraction for low zenith angles was probably higher than that used in the simulations. This could explain some underestimation of canopy reflectance in the visible. However, clumping features are usually expected to decrease the reflectance of multiple scattering (Nilson, 1991).
4. The underestimate of reflectance in the hot-spot direction could also be due to the calculation of the bidirectional gap fraction. Bidirectional gap fraction models have seldom been evaluated through direct measurements. This could be done by using hemispherical photographs (Andrieu et al. 1995).

CONCLUSION

The hotspot and the specular component of leaf reflectance are particularly important features that should be considered when calculating the bidirectional reflectance of crops characterized by broad and glossy leaves, such as sugar beets.

For this reason, reflectance of diffuse sky radiance should not be calculated from the two-stream approximation. Under clear sky conditions, the best approximation was to consider that all the light comes from the sun direction. Numerical integration may be useful for short wavelengths if the diffuse fraction is large and the directional distribution for skylight is properly approximated. Integration could be performed by using a relatively small number of directions, because of the smooth shape of canopy bidirectional reflectance.

The model satisfactorily estimated sugar beet reflectance for a wide range of canopy structures, background reflectances, leaf optical properties, and sun-sensor geometries. However, a significant underestimation occurred in two cases: 1) at all wavelengths for sun-sensor geometries close to the hot spot, and 2) in the near infrared, for sun-sensor geometries opposite to the hot spot. In both cases, the underestimation increases for large sun zenith angles.

From a practical point of view, the model gave quite accurate estimates of reflectance for the range of sun-sensor geometries corresponding to the acquisition of remote-sensing data by Earth observation satellites. This is satisfactory if one considers that the structure of sugar beet canopies departs strongly from the basic assumptions considered in that type of simple model.

Several factors may have contributed to the underestimations for sun-sensor geometries about the hot-spot or the specular region. Approximations exist in the computation of first-order scattering and of multiple scattering. However, there were striking similarities in the conditions of view-sensor geometry leading to underestimation for the near-infrared and the visible wave bands. Thus we believe that it would be of interest to further evaluate the calculation of parameters important for the first-order scattering, such as the directional and bidirectional gap fraction and the approximation of leaf phase function.

Field data were collected as part of the collaborative work by the Biophysical Analysis Research Group. Many thanks to J. Clark, M. Danson, J. Eastwood, J. F. Hanocq, and K. Jaggard, who contributed to the experiments. We acknowledge the following organizations for financial support: Programme National de Télétection Spatiale, INRA Direction des Relations Internationales, Natural Environmental and Research Council, Agriculture and Food Research Council, The British Council, Sugar Beet Research and Education Committee, and Sheffield University.

REFERENCES

Andrieu, B., Kiriakos, S., and Jaggard, K. W. (1992), Estimation de la concentration en chlorophylle par mesure de la reflectance des feuilles ou par analyse numérique de photographies de feuilles prises en laboratoire, *Agronomie* 12:477–485.

Andrieu, B., Sohbi, Y., and Ivanov, N. (1995), A direct method to estimate bi-directional gap fraction of vegetation canopies, *Remote Sens. Environ.* 50(1):61–66.

Baret, F., Andrieu, B., and Steven, M. (1993), Gap frequency and canopy architecture of sugar-beet and wheat crops, *Agric. For. Meteorol.* 65:261–279.

Breece, I. I. I. and Holmes, R.A. (1971), Bi-directional scattering characteristics of healthy green soybean and corn leaves in vivo, *Appl. Opt.* 10(1):119–127.

Campbell, G. S. (1986), Extinction coefficient for radiation in plant canopies calculated using an ellipsoidal inclination angle distribution, *Agric. For. Meteorol.*, 36:317–321.

Govaerts, Y., Jacquemoud, S., Verstraete M., and Ustin L. (1996), Three-dimensional radiation transfer modeling in a dicotyledon leaf, *Appl. Opt.*, 35(33):6585–6598.

Hodanova, D. (1972), Structure and development of sugar beet

canopy, I leaf area–leaf angle relations, *Photosynthetica* 6(4):401–409.

Jacquemoud, S. (1993), Inversion of the PROSPECT+SAIL canopy reflectance model from AVIRIS equivalent spectra, *Remote Sens. Environ.* 44:281–292.

Jacquemoud, S., and Baret, F. (1990), PROSPECT: A model of leaf optical properties spectra, *Remote Sens. Environ.* 34:75–91.

Jacquemoud, S., Baret F., Andrieu B., Danson M., and Jaggard, K. (1995), Extraction of vegetation biophysical parameters by inversion of the PROSPECT+SAIL model on sugar beet canopy reflectance data: application to TM and AVIRIS sensors, *Remote Sens. Environ.* 52:3,163–172.

Kuusk, A. (1985), The hot-spot effect of a uniform vegetative cover, *Sov. J. Rem. Sens.* 3(4):645–658.

Kuusk, A. (1991), The hot-spot effect in plant canopy reflectance, In *Photon Vegetation Interaction*, (R. B. Myneni and J. Ross Eds.), Springer-Verlag, Berlin, pp. 140–159.

Kuusk A. (1994), A multispectral canopy reflectance model, *Remote Sens. Environ.* 50:75–82.

Lang, A. R. G. (1993), Cauchys theorems and estimation of surface areas of leaves, needles and branches, In *Crop Structure and Light Microclimate* C. (Varlet-Grancher, R. Bonhomme, and H. Sinoquet. Eds), INRA, Paris, pp. 175–182.

Marshak A. L. (1989), Consideration of the effect of hot spot for the transport equation in plant canopies. *J. Quant. Spectros. Radiat. Transfer*, 42:615–630.

Myneni , R. B. and Kanemasu, E.T. (1988), The hot spot of vegetation canopies. . *J. Quant. Spectrosc. Radiat. Transfer* 40:165–168.

Nilson, T. (1971), A theoretical analysis of the frequency of gaps in plant stands, *Agric. Meteorol.* 8:25–38.

Nilson, T. (1991), Approximate analytical methods for calculating the reflection functions of leaf canopies in remote sensing applications, In *Photon-Vegetation Interactions*, (R. B. Myneni and J. Ross, Eds), Springer-Verlag, Berlin, pp. 163–189.

Qin, W. (1993), Modelling bi-directional reflectance of multicomponent vegetation canopies, *Remote Sens. Environ.* 46:235–245.

Qin, W., and Jupp D. L. B. (1993), An analytical and computationally efficient reflectance model for leaf canopies. *Agric. For. Meteorol.*, 66:31–64.

Qin, W. and Xiang, Y. (1994) On the hotspot effect of leaf canopies: modeling study and influence of leaf shape, *Remote Sens. Environ.* 50:95–106.

Ross, J. K. (1981), *The Radiation Regime and the Architecture of Plant Stands*, Junk Pub., The Hague, Netherlands.

Ross, J. K., and Marshak, A. (1989), The influence of leaf orientation and the specular component of leaf reflectance on the canopy bidirectional reflectance, *Remote Sens. Environ.* 27:251–260.

Sanz, C. (1994), Mesure et modélisation de la variation directionnelle des propriétés optiques des feuilles. *Mémoire de DEA*, AGTS, Université de Toulouse III, 30pp.

Vanderbilt, V. C., and Grant, L. (1985), Plant canopy specular reflectance model, *IEEE Trans. Geosci. Remote Sens.*. GE-23:722–730.

Verhoef, W. (1984), Light scattering by leaf layers with application to canopy reflectance modeling: the SAIL model, *Remote Sens. Environ.* 6:125–184.

Verhoef, W. (1985), Earth observation modeling based on layer scattering matrices, *Remote Sens. Environ.* 17:165–178.

Walter-Shea, E. A., Norman, J. M., Blad, B. L. (1989), Leaf bidirectional reflectance and transmittance in corn and soybean, *Remote Sens. Environ.* 29:161–174.